AMPP™
ANNUAL CONFERENCE + EXPO
MARCH 6–10, 2022 | SAN ANTONIO, TEXAS

Factors in Galvanic Corrosion between Steel and Iron Sulfides in Acidic Solutions

Payman Sharifi Abdar, Bruce Brown, Srdjan Nesic
Institute for Corrosion and Multiphase Technology, Ohio University
342 W State Street
Athens, Ohio, 45701
USA

ABSTRACT

With the increase in producing sour oil and gas fields in the world, mitigation of production related failures due to H_2S corrosion is a key challenge. In H_2S environments, localized corrosion is the type of attack which contributes to the most failures in oilfields. The main cause of localized attack is the galvanic coupling between steel and iron sulfide corrosion products due to their electrical conductivity. However, the mechanism of the galvanic coupling between steel and iron sulfides and the effect of experimental parameters on it, have not been unraveled yet. The present study investigates the effect of three different experimental parameters: iron sulfide type, cathode to anode surface ratio, and salt concentration, on the galvanic coupling between steel and iron sulfides in acidic solutions. Pyrite and pyrrhotite were selected as iron sulfide specimens since these corrosion products have been mostly found when localized corrosion of mild steel was observed in sour environments. The results show that the cathodic current of pyrrhotite was an order of magnitude higher than the cathodic current of pyrite, leading to a higher galvanic current as well as a higher galvanic potential for coupled steel-pyrrhotite compared to coupled steel-pyrite. In addition, it was found that the increase of cathode to anode surface area ratio as well as the increase of salt concentration to some extent, increased the galvanic current for the coupled materials.

Key words: H_2S Corrosion, Localized Attack, Galvanic Coupling, Iron Sulfides, Pyrite, Pyrrhotite, Mild Steel

INTRODUCTION

H_2S corrosion, also known as sour corrosion, is one of the most researched types of metal degradation in oil and gas transmission pipelines requiring a wide range of environmental conditions and detailed surface analysis techniques. This is because localized or pitting corrosion is known to be the main type of corrosion failure in sour environments which caused 12% of all oilfield corrosion incidents according to a report from 1996.[1] Therefore, control and reduction of this type of corrosion could prevent such failures in oil and gas industries, and significantly enhance asset integrity while reducing maintenance costs as well as eliminating environmental damage. The unpredictability of pitting corrosion in sour media

is a complicated challenge in this area as several factors, such as the nature of the corrosion products and the contribution of galvanic coupling, play a role in this type of corrosion.[2,3]

Galvanic coupling between iron sulfides and mild steel is thought to be an important mechanism leading to localized corrosion on steel surface in H_2S environments. In one of the premiere studies done in this area, Ning et al.[3] showed that galvanic coupling between pyrite and steel could cause severe localized corrosion by designing a set of experiments to separate the influence of galvanic coupling from the chemical effects on the localized corrosion of steel in H_2S environments. In these experiments, the presence of pyrite particles on a API 5L X65 steel surface in 1 wt% NaCl solution at pH 4, 25 °C, 0.1 bar pH_2S for one week, resulted in severe localized attacks on the surface of steel. In the exact same experimental conditions, when a nylon mesh with a 60 μm pore size was placed between pyrite particles and the steel surface, no localized attack was observed. This study revealed that the localized corrosion of steel in presence of iron sulfides has an electrochemical nature, and thus proposed the galvanic coupling as the mechanism of these localized attacks.[3]

Hitherto, few studies have measured galvanic corrosion between iron sulfides and mild steel in order to verify the proposed mechanism and understand the effect of experimental parameters on it.[4,5,6,7] Navabzadeh[4] investigated the effect of different types of iron sulfides and showed that galvanic current between an API 5L X65 steel specimen and a pyrrhotite specimen (an X65-pyrrhotite couple) is slightly higher than X65-pyrite couple in CO_2, H_2S and N_2 sparged solutions at pH 3, 4, and 5.[4] In another study, Tjelta et al.[5] showed that iron sulfides act as cathodes when coupled to API 5L X65 mild steel. They compared the effect of various types of iron sulfides and concluded that pyrite has the largest ability to polarize steel but pyrrhotite can produce the largest galvanic coupling current.[5] Finally, Yepez et al.[6] studied the effect of different iron sulfides when coupled to steel and showed that corrosion current of steel was increased due to coupling to both pyrite and pyrrhotite. Although these studies confirm that galvanic coupling significantly affects the corrosion rate of steel, the results of these studies are in some cases contradictory and the experimental setups were not well designed, e.g., surface area of electrodes were not specified. In addition, the lack of investigation on the effect of various experimental conditions and surface analysis related to the iron sulfides chemistry resulted that no detailed mechanism has been proposed for the galvanic coupling between steel and iron sulfides.

The present study aims to investigate the effect of influential experimental parameters: type of iron sulfide, cathode to anode surface ratio, and salt concentration, on the galvanic corrosion of steel due to coupling to iron sulfides. Understanding the impact of these factors could lead to revealing the proper mechanism of galvanic corrosion of steel in sour environments. Pyrite and pyrrhotite were selected as these corrosion products have been mostly found when localized attack of mild steel was observed in presence of H_2S, according to previous studies[8,9]. Cathode to anode surface ratio is another important factor in this process as the high porosity of iron sulfides formed on the surface of steel could increase the surface area of iron sulfides (cathode) to one or two order of magnitudes higher than the steel (anode). This high ratio could significantly amplify the effect of galvanic coupling and intensify the localized attack. Salt concentration is also an influential factor since higher salt concentration increases galvanic current by facilitating the electron transfer in solution. It is worth noting that all the experiments will be performed in acidic solutions because the presence of H_2S, as another influential factor, was shown in the literature[10] to significantly effect both anodic and cathodic reactions on steel surface leading to a more complex system. Therefore, it is reasonable to eliminate the effect of H_2S in this stage in order to clearly understand the importance of other influential factors. It should be mentioned that the effect of H_2S will be studied during the final phase of this project and the results will be presented in future publications.

EXPERIMENTAL PROCEDURE

An experimental setup was designed for this study in which the surface areas of specimens are specified. The surface areas were selected for the investigation of the effect of cathode to anode ratio of around one and two orders of magnitude. API 5L X65 and iron sulfides specimens (pyrite, and pyrrhotite) with two different surface areas, (0.196 and 0.0177 cm^2) for steel and (0.196 and 1.613 cm^2) for iron sulfides, were cut to the right shape. The iron sulfide specimens were attached to a wire using silver conductive paste, and then were embodied in epoxy. Mineral pyrite and pyrrhotite were purchased from Ward's

Science, then powdered by pestle and mortar and analyzed by XRD which showed high purity of the samples. These two electrodes were placed on a holder with a set distance of two centimeters apart as shown in Figure 1. A platinum (Pt) mesh counter electrode was placed in the middle of these two electrodes. Also, a saturated Ag/AgCl reference electrode (RE) was kept between the Pt counter electrode (CE) and the working electrode (WE) for corrosion rate and potentiodynamic measurements. The electrodes are facing each other so that the current flow would be uniform in this design. Figure 1 shows an image of the arrangement of the electrodes in a two-liter glass cell.
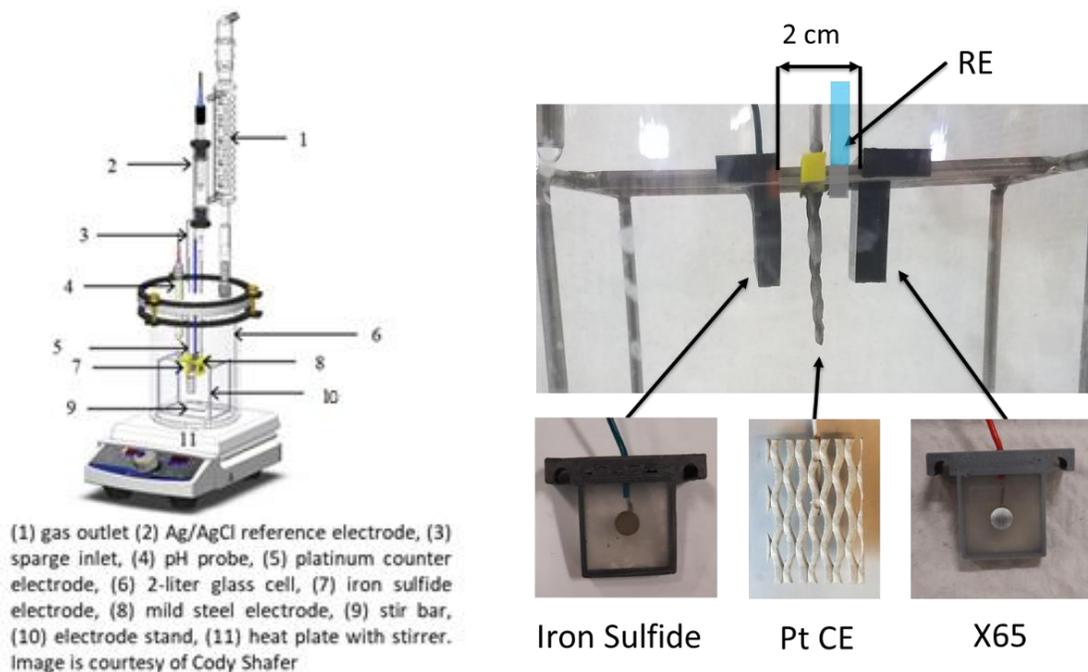

(1) gas outlet (2) Ag/AgCl reference electrode, (3) sparge inlet, (4) pH probe, (5) platinum counter electrode, (6) 2-liter glass cell, (7) iron sulfide electrode, (8) mild steel electrode, (9) stir bar, (10) electrode stand, (11) heat plate with stirrer. Image is courtesy of Cody Shafer

Figure 1. Overview of the experimental setup (left), and image of the electrochemical cell (right)

For the galvanic coupling measurements, steel was coupled to iron sulfide for two hours during which galvanic current and galvanic potential were measured using zero resistance ammeter (ZRA) method. In order to observe the behavior of steel specimen during galvanic measurements, the open circuit potential (OCP) and the corrosion rate of uncoupled steel, using linear polarization resistance (LPR) method, were measured. For this purpose, the steel specimen was uncoupled from iron sulfide every 30 minutes during the galvanic measurements and re-coupled after OCP and LPR measurements. In addition, potentiodynamic sweeps were also measured on both electrodes at the end of the two-hour galvanic measurements. Solution resistance was also measured using electrochemical impedance spectroscopy (EIS) and compensated for the measurements. The pH of solution was kept at 5, using HCl and NaOH, in order to mimic the pH of real conditions of oil and gas pipelines. In total, six experiments were conducted in this study in order to investigate the effect of three experimental parameters. The test matrix is shown in Table 1.

Table 1. Test matrix

Parameter	Conditions	
Material	X65, Pyrite	X65, Pyrrhotite
Steel size	5 mm D (0.196 cm^2), 1.5 mm D (0.0177 cm^2)	
Iron sulfide size	5 mm D (0.196 cm^2), 1.27 cm ×1.27 cm (1.613 cm^2)	
Cathode/Anode ratio	1, 8.2, 91.1	
Temperature	30°C	
Electrolyte	0.1 wt.%, 1 wt.%, 10 wt.% NaCl	
Sparge gas	N$_2$	
Total pressure	1 bar	
pH	5.0 ± 0.1	
Exposure time	2 hours	
Electrochemical techniques	OCP, EIS, LPR, ZRA, Potentiodynamic sweep	

RESULTS

Effect of Iron Sulfide Type

The coupled potential and current were measured using ZRA method on two different iron sulfides, i.e., pyrite and pyrrhotite, and the results are plotted in Figure 2. The blue line represents the corrosion potential (Figure 2A) and corrosion current (Figure 2B) of uncoupled steel which was measured every 30 minutes and shown as points. As observed in Figure 2A, the increase in mild steel potential when coupled to pyrite was around 10 mV, while it was around 100 mV when coupled to pyrrhotite. Therefore, pyrrhotite showed the ability to significantly polarize the steel. The coupled pyrrhotite-steel current was also significantly increased by an order of magnitude due to the coupling while the coupled pyrite-steel current was less than the corrosion rate of uncoupled steel (Figure 2B). The observed different behavior could originate from the different nature of pyrite and pyrrhotite.

It is worth noting that the spikes observed every 30 minutes in the data was due to the disconnection and reconnection of the electrodes at these times for measuring the potential and corrosion current of uncoupled steel. When reconnecting the electrodes, the spikes appeared due to the polarization of the mild steel at the beginning of the coupling.
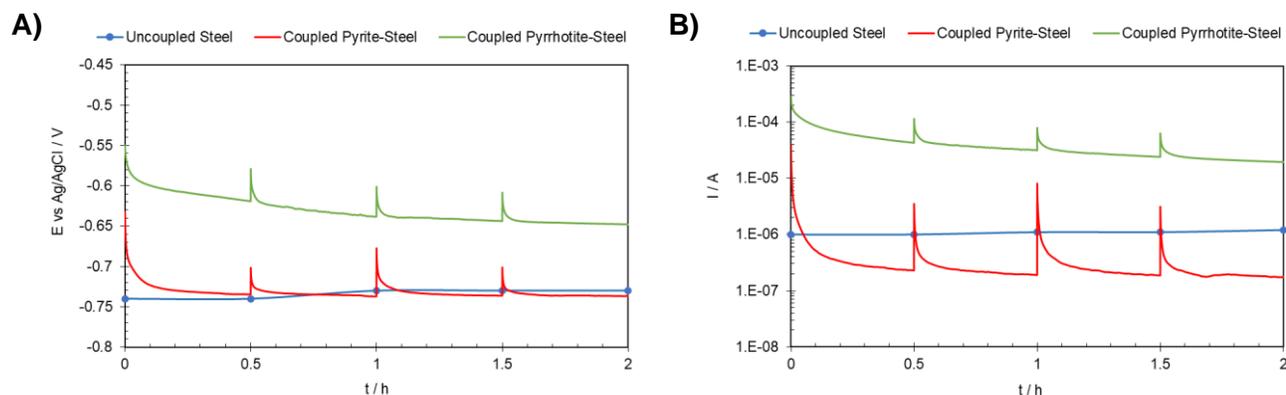

Figure 2. A) potential, B) current of steel when coupled to pyrrhotite and pyrite at 30 ˚C, 1 wt.% NaCl, pH 5, cathode/anode ratio = 1

In order to investigate the different behavior of pyrite and pyrrhotite on galvanic corrosion, the cathodic current of these iron sulfides have been measured and plotted in Figure 3. It can be seen that the cathodic current of pyrrhotite is much greater than pyrite which leads to the higher rate of galvanic current in a same condition. The total cathodic current (black dotted lines) was calculated by adding the cathodic current of steel to that of pyrrhotite or pyrite. The intersection of total cathodic current and the anodic current of steel results in the galvanic potential and total corrosion current of steel. It should be emphasized that the galvanic current is not the intersection of cathodic current of iron sulfides and anodic current of steel. The galvanic current is indeed the intersection of cathodic current of iron sulfides at the galvanic potential. It is also worth noting that the total current in the case of pyrrhotite was almost equal to the cathodic current on pyrrhotite surface due to its very high values as compared to the cathodic current of steel. Also, the anodic current of the iron sulfides has been disregarded since their values are much lower than anodic current of steel. Based on the above discussion, it can be found from Figure 3 that the results of potentiodynamic sweeps' analysis are consistent with the galvanic measurements, and the high cathodic current of pyrrhotite resulted in a high galvanic current in this condition.
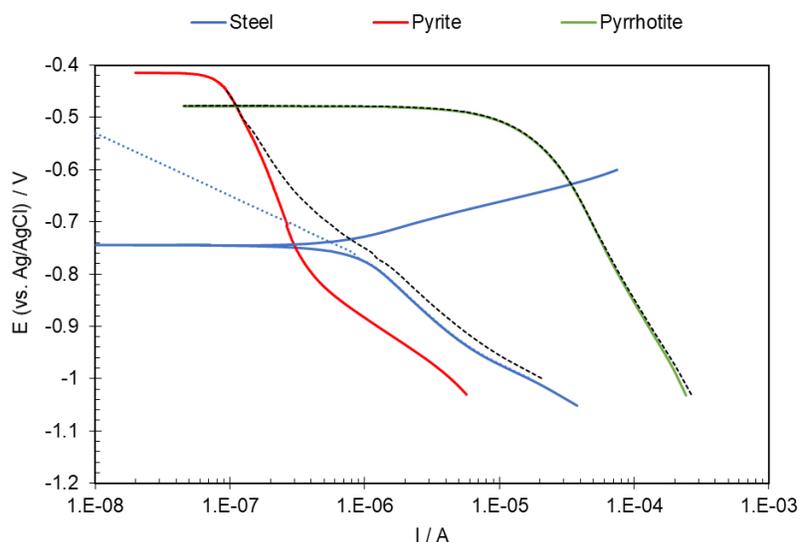

Figure 3. Potentiodynamic sweeps on X65 mild steel, pyrite and pyrrhotite at 30 ˚C, 1 wt.% NaCl, pH 5, and cathode/anode surface area ratio = 1 (black dotted lines = total cathodic currents, and blue dotted line = calculated cathodic current on steel).

For the abovementioned experiments, the corrosion rates of coupled steel-pyrite and steel-pyrrhotite were calculated using galvanic coupling measurements (Figure 2) and presented in Figure 4. The corrosion rate of uncoupled steel was also calculated from LPR measurements which were done every 30 minutes. All the corrosion rates were calculated using the average value during two-hours experiments. Based on these results, it can be concluded that pyrite does not significantly increase the corrosion rate of steel due to galvanic coupling, while pyrrhotite could increase the corrosion rate of steel by an order of magnitude due to galvanic coupling.
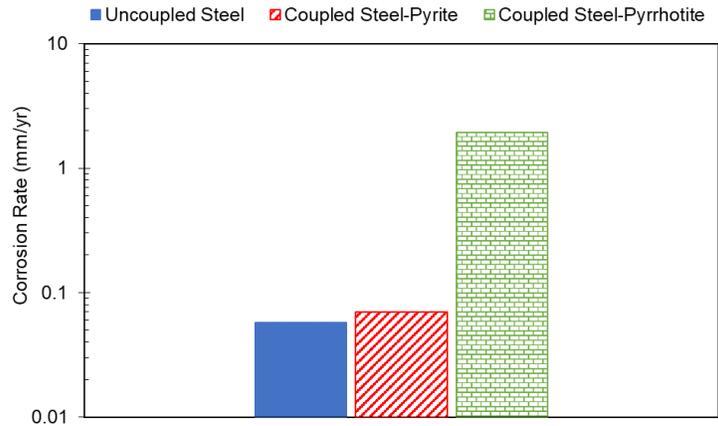
Figure 4. Calculated corrosion rates of uncoupled and coupled X65 mild steel at 30 ˚C, 1 wt.% NaCl, pH 5, cathode/anode surface area ratio = 1.

Effect of Cathode to Anode Surface Area Ratio

The effect of cathode to anode surface area ratio was investigated by changing the surface areas of steel and iron sulfides in order to increase it by roughly one and two orders of magnitude. All other experimental conditions remained unchanged. Figure 5 compares the galvanic potentials due to coupling with different cathode to anode surface ratios for pyrite and pyrrhotite. In both cases, the coupled potential increased with respect to the cathode to anode surface area ratio showing the influence of iron sulfides with the larger surface area for polarizing the steel. Larger cathodes (iron sulfides) would increase the cathodic current of iron sulfides leading to the increase in coupled potential.
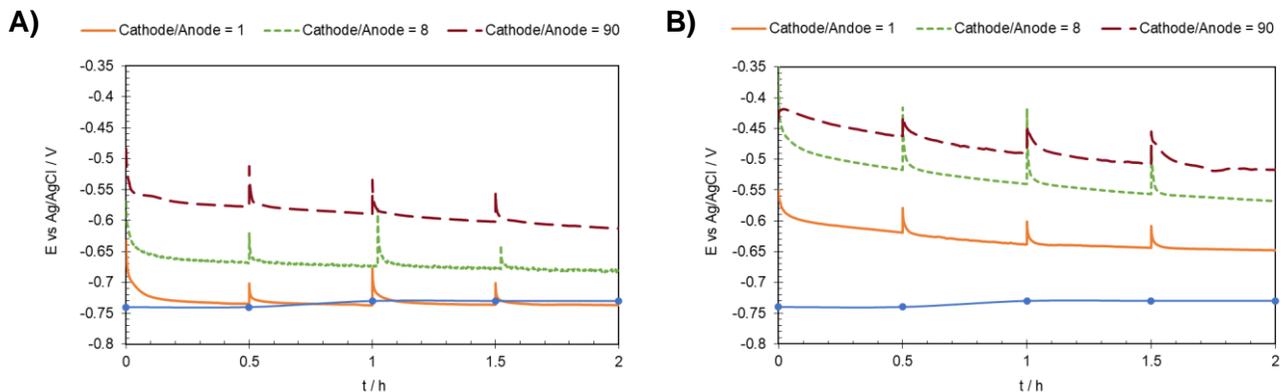

Figure 5. The effect of cathode to anode surface ratio on the galvanic potential of steel when coupled to A) pyrite, and B) pyrrhotite at 30 ˚C, 1 wt.% NaCl, and pH 5. The solid blue line shows the open circuit potential of uncoupled steel.

Galvanic current density was also compared for different cathode to anode surface area ratios. Current density was used in this case instead of current as the steel surface areas were different. The results in Figure 6 show that the current density was increased around one and two orders of magnitude by increasing the cathode to anode surface area ratio from one to 8.2 and 91.1. The increase in current density was due to the increase of cathodic current because of the larger cathodic surface area.
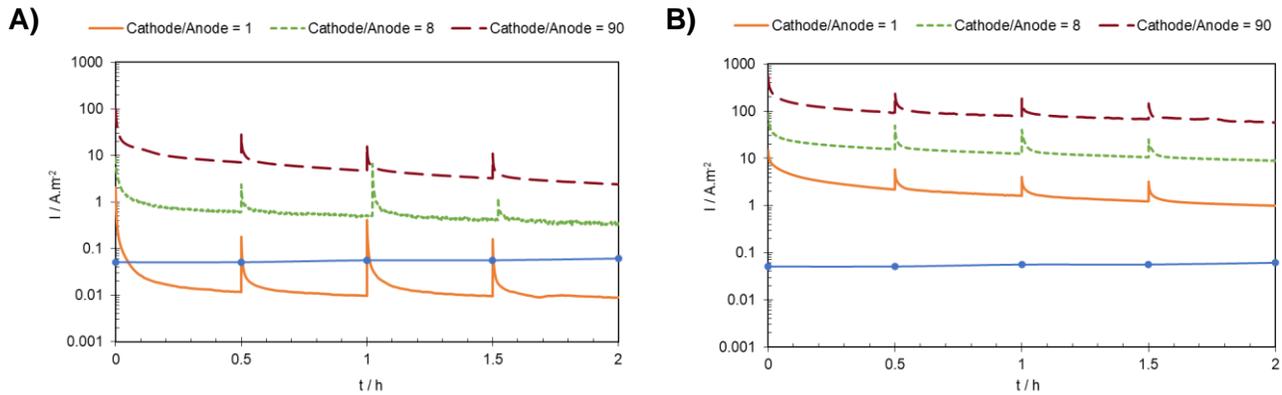
Figure 6. The effect of cathode to anode surface ratio on the galvanic current of steel when coupled to A) pyrite, and B) pyrrhotite at 30 ˚C, 1 wt.% NaCl, and pH 5. The solid blue line shows the corrosion current of uncoupled steel.

Same as the previous case, corrosion rates were calculated for different cathode to anode surface area ratios. As seen in Figure 7, by increasing the cathode to anode surface area from 1 to 8.2 to 91.1, the galvanic corrosion rates of steel due the coupling to both pyrite and pyrrhotite were increased by approximately one and two orders of magnitude, respectively.
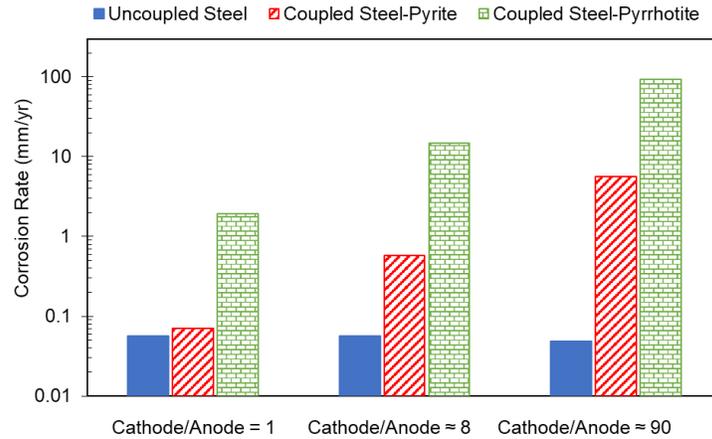
Figure 7. The effect of cathode to anode surface area ratio on corrosion rates of uncoupled and coupled X65 mild steel at 30 ˚C, 1 wt.% NaCl, pH 5

Effect of Salt Concentration

Finally, the effect of salt concentration was investigated by changing the salt concentrations to 0.1 and 10 wt.% NaCl. Figure 8 compares the galvanic current for both pyrite and pyrrhotite cases. It should be mentioned that the change of corrosion current of uncoupled steel due to the change in salt concentration was neglected as only a minor effect was found in these experiments. The increase in salt concentration from 0.1 wt.% to 1 wt.% NaCl increases the galvanic current for pyrrhotite, but further increase to 10 wt.% shows only a very minor effect. Changing salt content does not change the galvanic current in pyrite. One reason for this behavior is that conductivity might not be the rate limiting factor for the case of low current in the presence of pyrite or with 10 wt.% NaCl of pyrrhotite. In other words, as the current is very low in the case of pyrite, even a solution with 0.1 wt.% salt is able to transfer the ions needed for such a low current. Therefore, increasing salt concentration does not affect the rate of ions transfer.
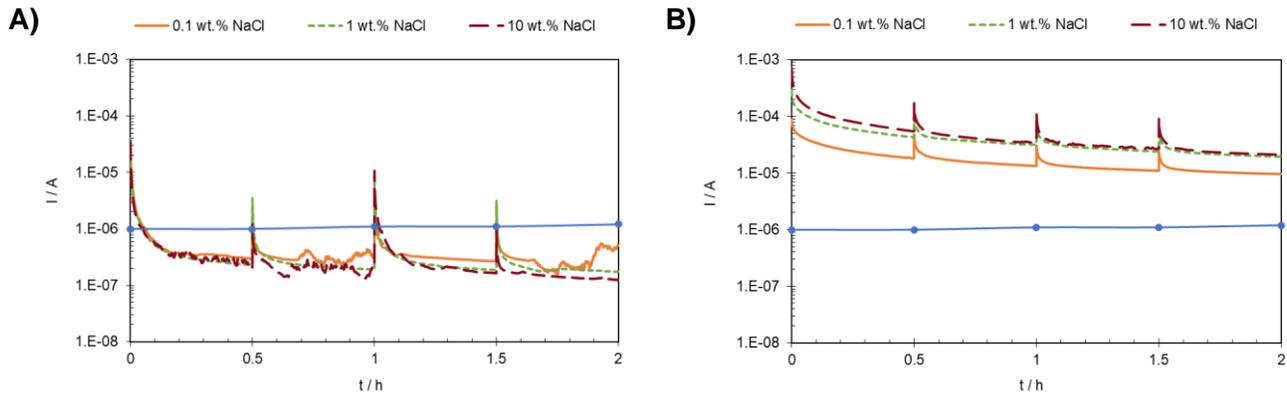
Figure 8. The effect of salt concentration on the galvanic current of steel when coupled to A) pyrite, and B) pyrrhotite at 30 ˚C, pH 5, and cathode/anode surface area ratio = 1. The solid blue line shows the corrosion current of uncoupled steel.

Corrosion rates were calculated for different salt concentrations as shown in Figure 9. The higher salt concentration resulted in a higher corrosion rate for mild steel coupled to pyrrhotite, while it did not affect the corrosion rate of steel due to coupling to pyrite. It can also be observed that increasing the salt content by 10 to 100 times did not increase the uncoupled corrosion rate by the same order of magnitude. As discussed previously, conductivity is not the only limiting factor in these cases.
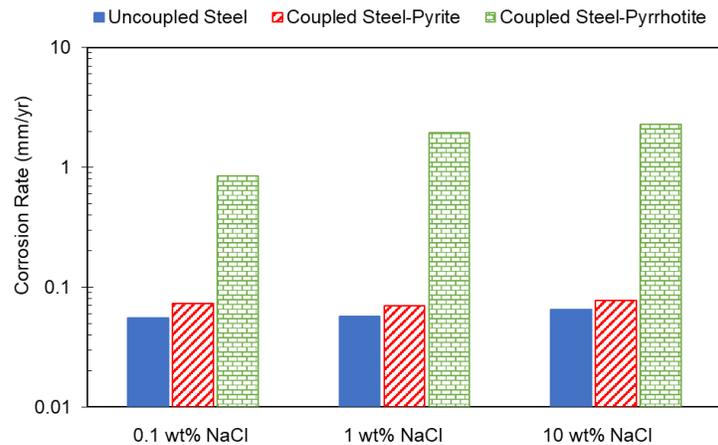

Figure 9. The effect of salt concentration on corrosion rates of uncoupled and coupled steel at 30 ˚C, pH 5, cathode/anode surface area ratio = 1

Finally, the effect of salt concentration was measured for the cathode to anode surface area ratio of 8.2 as the effect of salt concentration was more observable with a higher cathode to anode surface area ratio due to the higher current in this condition. Figure 10 shows the galvanic corrosion measurements for different salt concentrations in this condition. Again, increase of salt concentration from 0.1 wt.% to 1 wt.% NaCl increased the galvanic current for both electrodes, but further increase to 10 wt.% shows only a very slight effect. This confirms that conductivity was not a rate determining factor when salt concentration was very high.
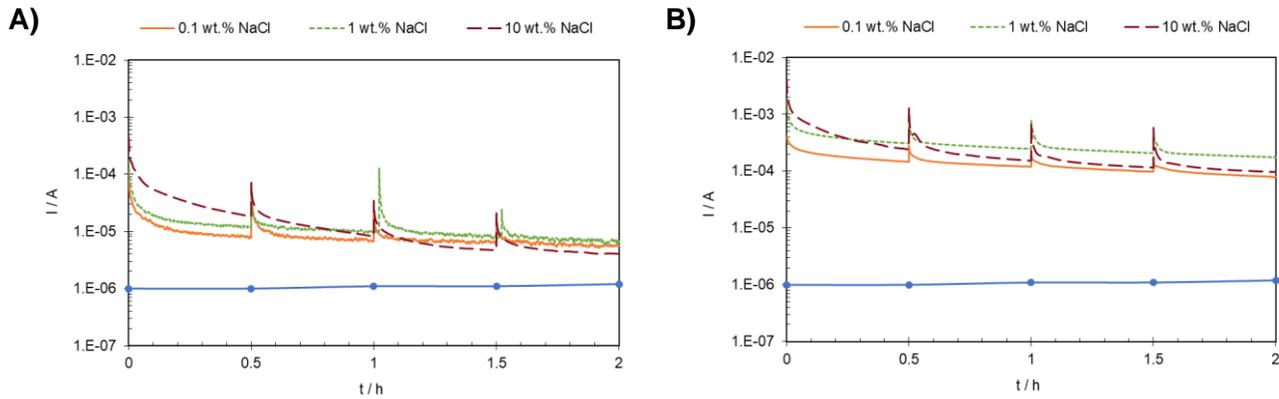
Figure 10. The effect of salt concentration on the galvanic current of steel when coupled to A) pyrite, and B) pyrrhotite at 30 ˚C, pH 5, and cathode/anode surface area ratio = 8. The solid blue line shows the corrosion current of uncoupled steel.

The corrosion rates were also calculated for this condition and shown in Figure 11. The corrosion rates increased by increasing the concentration from 0.1 wt.% to 1 wt.%. This increase is more distinct in the case of steel-pyrrhotite couple due to its higher galvanic current. As discussed before, increasing the salt concentration to 10 wt.% does not increase the corrosion rates as conductivity was not the limiting factor in these conditions.
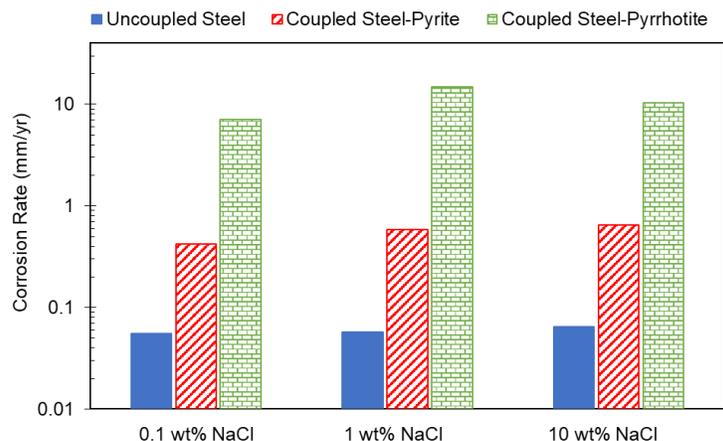

Figure 11. The effect of salt concentration on corrosion rates of uncoupled and coupled steel at 30 ˚C, pH 5, cathode/anode surface area ratio = 8.

CONCLUSIONS

- In these experimental conditions, when cathode to anode surface area ratio was one, pyrite did not significantly increase the corrosion rate of steel while pyrrhotite increased the corrosion rate of steel by an order of magnitude. This behavior was related to the higher cathodic current on the pyrrhotite surface.
- Increasing the cathode to anode surface area by one and two orders of magnitude increases the galvanic corrosion rate of steel by the same order in the presence of both pyrite and pyrrhotite.
- Increasing the salt concentration from 0.1 wt.% to 1 wt.% NaCl increased the galvanic corrosion of steel for both cases. However, very high salt concentrations i.e., 10 wt.% NaCl did not increase the galvanic corrosion.

ACKNOWLEDGEMENTS

REFERENCES

1. M.B. Kermani; D. Harrop, "The Impact of Corrosion on Oil and Gas Industry." *SPE Production & Facilities* 1996, *11* (03), 186–190
2. J. Kvarekval, "Morphology of Localized Corrosion Attacks in Sour Environment." CORROSION/2007; Paper No. 7659.
3. J. Ning, "The Role of Iron Sulfide Polymorphism in Localized Corrosion of Mild Steel" Dissertation, Ohio University, 2016.
4. S. Navabzadeh Esmaeely, "Galvanic Localized Corrosion of Mild Steel under Iron Sulfide Corrosion Product Layers" Dissertation, Ohio University, 2018.
5. M. Tjelta; J. Kvarekval, "Electrochemistry of Iron Sulfide and Its Galvanic Coupling to Carbon Steel in Sour Aqueous Solutions", CORROSION/2016; Paper No. 7478.
6. O. Yepez; N. Obeyesekere; J. Wylde, "Study of Sour Corrosion Mechanism under Controlled pH", CORROSION/2016; Paper No. 7795.
7. P. Sharifi Abdar, B. Brown, S. Nesic, "Factors in Galvanic Coupling Between Steel and Iron Sulfides", ECS Meeting Abstracts, No. 9, p.565, 2021
8. S. Gao, P. Jin, B. Brown, D. Young, S. Nesic, M. Singer, "Corrosion Behavior of Mild Steel in Sour Environments at Elevated Temperatures", Corrosion, Vol. 73, No. 8, pp. 915-926, 2017
9. J. Ning, Y. Zheng, B. Brown, D. Young, S. Nesic, "The Role of Iron Sulfide Polymorphism in Localized H_2S Corrosion of Mild Steel", Corrosion, Vol. 73, No. 2, pp. 155-168, 2017
10. P. Sharifi Abdar, M. Bagheri Hariri, A. Kahyarian, S. Nesic, "A Revision of mechanistic modeling of mild steel corrosion in H_2S environments", Electrochimica Acta, 382 (2021): 138231